Assessment of an Assumed Strain-based Quadrilateral Membrane Element

Abdelhak Kherfi
Laboratory of Development in Mechanics and Materials (LDMM)
University of Djelfa
Djelfa, Algeria
a.ak.k65@gmail.com

Khelifa Guerraiche
Mechanical Engineering Department, Faculty of Technology, University of Batna 2, Batna, Algeria
NMISSI Laboratory, Faculty of Science and Technology, Biskra University, Biskra, Algeria
guer.khelifa@yahoo.com

Kamel Zouggar
Laboratory of Mechanics of Structures and Solids (LMSS)
Faculty of Technology, Djillali Liabès University of Sidi Bel-Abbès, Sidi Bel Abbès, Algeria
zouggarkamel.zk@gmail.com

Received: 6 July 2022 | Revised: 31 July 2022 | Accepted: 4 August 2022

Abstract-This paper describes the development of a simple quadrilateral strain-based element for plane stress and strain problems. This element has five nodes, four located at its corners and one at the center. Each of the four corner nodes had two essential external degrees of freedom (u, v), while the center node had three degrees of freedom (u, v, ө); the static condensation method was used for the internal node. This element was used for both linear and dynamic analysis. Its performance was assessed using a variety of membrane and axisymmetric analysis problems. The obtained results demonstrated the good performance and accuracy of the proposed element.

Keywords-strain approach; drilling rotation; quadrilateral element; linear analysis; dynamic analysis; axisymmetric

I. INTRODUCTION

Numerical methods, such as finite elements, finite volumes, finite differences, and discrete element methods are powerful and efficient computational tools for solving engineering problems. However, the finite element method is the most popular because of its robust mathematical basis and applicability, which is reflected in its extensive use in various applications [1-3]. In [4], the linear (constant-strain) triangle and the bilinear rectangle were formulated, based on the displacement approach in standard elements, whereas in [5] the standard bilinear quadrilateral was produced. They have been extensively used as plane-stress, plane-strain, and axisymmetric-solid models for two-dimensional structures. However, computational experience soon showed that these elements are excessively stiff for problems where linear strain gradients dominate the response. Furthermore, over-rigidity grows rapidly as the rate of aspect degrades. These behaviors are referred to as mesh distortions and bending problems.

Much effort has been put into improving these or creating new simple elements. Some studies showed that other strategies, such as hybrid stress elements [6-8], assumed strain or enhanced assumed strain elements [9-11], quasi-conforming elements [12, 13], and generalized conforming elements [14-16] provide special advantages compared to classic finite elements. The development of efficient and straightforward finite elements to analyze structures is a primary motivation for scientific research in solid mechanics. A class of elements was developed using the strain-based approach. This approach produces displacement fields enriched by higher-order terms, without the necessity of introducing non-essential degrees of freedom, hence obtaining elements with more accurate results on displacements. The resulting elements from this approach are free from shear locking and parasitic shear. The state of strains for this approach is composed of rigid body motions, constant strains, and higher-order strains. This approach was used in [17] for curved structures, and it was extended for plan elasticity [11, 18-21]. A summary of this early work was presented in [22, 23], with three-dimensional elasticity problems [24-26], plate bending [9, 27-30], and shell structures [31-34]. Other studies presented the treatment of non-linear problems [31, 35-36], composite materials [37], functionally graded plates [29, 38], and fracture mechanics [39]. These elements are stable and have good efficiency, and the strain approach is very practical for the development of robust finite elements which are insensitive to common problems such as mesh sensitivity and different locking problems.

This paper presents a quadrilateral element based on strain formulation. The proposed element has two degrees of freedom (u, v) at each of the corner nodes. Moreover, to enrich the strain field (ε_x, ε_y, and γ_{xy}) of the element, an internal node was introduced with three degrees of freedom (u, v, θ) to improve accuracy and reduce computational effort for the analysis of the plane structure, which will be subsequently eliminated by static condensation [11, 18]. After condensation, the element becomes a simple four-node quadrilateral element. Each node contains the two essential translational degrees of freedom, and hence the element is free of any parasitic and shear problems and is insensitive to mesh distortion. Various numerical problems (plane elasticity, axisymmetric, and dynamics) verified the high accuracy and efficiency of the proposed element compared to other existing plane elements.

Corresponding author: Abdelhak Kherfi

II. Formulation of the Developed Element

The proposed Strain Based Five Node (SBFN) element is quadrilateral with two degrees of freedom at each of the corner nodes, corresponding to two translations (u, v), and additional in-plane translations (u, v) associated with the rotation degree of freedom θ_z at the internal node, as shown in Figure 1.

A. *Case of Plane Elasticity*

The strain components relations and compatibility equation for plan elasticity are respectively given as:

$$\begin{cases} \varepsilon_x=\frac{\partial u}{\partial x} \\ \varepsilon_y=\frac{\partial v}{\partial x} \\ \gamma_{xy}=\frac{\partial u}{\partial y}+\frac{\partial v}{\partial x} \end{cases} \quad (1)$$

$$\frac{\partial^2\varepsilon_x}{\partial y^2}+\frac{\partial^2\varepsilon_y}{\partial x^2}-\frac{\partial^2\gamma_{xy}}{\partial x\cdot\partial y}=0 \quad (2)$$

where u and v are the displacements in the x and y axes respectively, ε_x and ε_y are the normal strains, and γ_{xy} is the shear strain. The rigid body modes displacement field is determined by setting the three deformations in (1) to zero, followed by integration:

$$\begin{cases} u=a_1-a_3y \\ v=a_2+a_3x \\ \theta=a_3 \end{cases} \quad (3)$$

The following equation is used for the element's drilling degree of freedom:

$$\theta=\frac{1}{2}\left(\frac{\partial v}{\partial x}-\frac{\partial u}{\partial y}\right) \quad (4)$$

Figure 1 shows the geometry of the proposed SBFN element and the corresponding nodal displacements:

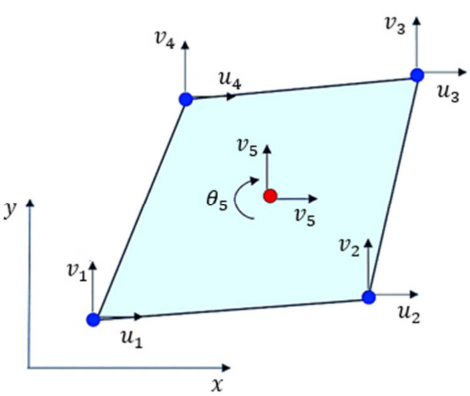

Fig. 1. The strain based five node element.

The SBFN element has eleven independent degrees of freedom, and therefore the displacement field should contain eleven independent constants. Since the three constants a_1, a_2, and a_3 represent the displacement field of the rigid body modes, as shown in (3), the remaining eight constants a_4, a_5,…,a_{11} denote the imposed strains of the elements that are expressed as:

$$\begin{cases} \varepsilon_x=a_4+a_5y+a_8x+\frac{a_{10}}{2}(x^2+y^2) \\ \varepsilon_y=a_6+a_7x-a_9y+\frac{a_{10}}{2}(x^2+y^2) \\ \gamma_{xy}=2a_{11}+2a_{10}(x^2-y^2+y-x+xy) \end{cases} \quad (5)$$

The strain functions for the present element, given above, satisfy the compatibility equation (2). These can be written in matrix form:

$$\{\varepsilon\}=[Q]\{a\} \quad (6)$$

where $[Q]$ presents the matrix relating the strain fields to the unknown constants, given by:

$$[Q]=\begin{pmatrix} 0 & 0 & 0 & 1 & y & 0 & 0 & x & 0 & \frac{x^2}{2}+\frac{y^2}{2} & 0 \\ 0 & 0 & 0 & 0 & 0 & 1 & x & 0 & -y & \frac{x^2}{2}+\frac{y^2}{2} & 0 \\ 0 & 0 & 0 & 0 & 0 & 0 & 0 & 0 & 0 & 2x^2+2xy-2x-2y^2+2y & 2 \end{pmatrix} \quad (7)$$

Integrating (5) and substituting (3), the final displacement functions can be obtained:

$$\begin{cases} u=a_1-a_3y+a_4x+a_5xy-\frac{y^2}{2}a_7+\frac{y^2}{2}a_8+\left(\frac{x^3}{6}+\frac{xy^2}{2}-\frac{2y^3}{3}+y^2\right)a_{10}+a_{11}y \\ v=a_2+a_3x-\frac{x^2}{2}a_5+a_6y+a_7xy-\frac{y^2}{2}a_9+\left(\frac{2x^3}{3}+\frac{yx^2}{2}-x^2+\frac{y^3}{6}\right)a_{10}+a_{11}x \\ \theta=a_3-a_5x+a_7y+a_{10}(x^2+y^2-y-x) \end{cases} \quad (8)$$

These can be written in matrix form as:

$$\{u\}=[T]\{a\} \quad (9)$$

where $[T]$ is expressed as:

$$[T]=\begin{pmatrix} [P] \\ [R] \end{pmatrix} \quad (10)$$

and:

$$[P]=\begin{pmatrix} 1 & 0 & -y & x & xy & 0 & -\frac{y^2}{2} & \frac{x^2}{2} & 0 & \frac{x^3}{6}+\frac{xy^2}{2}-\frac{2y^3}{3}+y^2 & y \\ 0 & 1 & x & 0 & -\frac{x^2}{2} & y & xy & 0 & -\frac{y^2}{2} & \frac{y^3}{6}+\frac{yx^2}{2}+\frac{2x^3}{3}-x^2 & x \end{pmatrix} \quad (11)$$

$$[R]=\begin{pmatrix} 0 & 0 & 1 & 0 & -x & 0 & y & 0 & 0 & x^2-x+y^2-y & 0 \end{pmatrix} \quad (12)$$

The nodal displacements and the vector coefficients $\{a\}$ are related as:

$$\{q_e\}=[C]\{a\} \quad (13)$$

where:

$$\{q_e\}=\{u_1,v_1,u_2,v_2,u_3,v_4,u_4,v_5,u_5,\theta_5\}^T \quad (14)$$

$$\{a\}=\{a_1,a_2,a_3,a_4,a_5,a_6,a_7,a_8,a_9,a_{10},a_{11}\}^T \quad (15)$$

where $[C]$ (11×11) is the matrix that relates nodal displacements to the constants (a_1 to a_{11}) as follows:

$$[C]=\begin{pmatrix} [P(x_1,y_1)] \\ [P(x_2,y_2)] \\ [P(x_3,y_3)] \\ [P(x_4,y_4)] \\ [P(x_5,y_5)] \\ [R(x_5,y_5)] \end{pmatrix} \quad (16)$$

From (13), the following can be obtained:

$$\{a\}=[C]^{-1}\{q_e\} \quad (17)$$

By substituting (17) into (6) and (9):

$$\{U\}=[P][C]^{-1}\{q_e\}=[N]\{q_e\} \quad (18)$$

and:

$$\{\varepsilon\}=[Q][C]^{-1}\{q_e\}=[B]\{q_e\} \quad (19)$$

where:

$$[N]=[P][C]^{-1};\ [B]=[Q][C]^{-1} \quad (20)$$

The stress-strain relationship is given by:

$$\{\sigma\}=[D]\{\varepsilon\} \quad (21)$$

where *[D]* is the elasticity matrix given in Appendix A for plane stress and plane strain, respectively. The procedures to obtain the element stiffness matrix, are:

The standard weak form for static can be expressed as:

$$\int_{V^e} \delta\{\varepsilon\}^T\{\sigma\}dV=\int_{V^e} \delta\{U\}^T\{f_v\}dV \quad (22)$$

By substituting (18), (19), and (21) into (22) we get:

$$\delta\{q_e\}^T\left(\int_{V^e} [B]^T[D][B]dV\right)\{q_e\}=\delta\{q_e\}^T\left(\int_{V^e} [N]^T\{f_v\}dV\right) \quad (23)$$

where:

$$[K_e]=\left(\int_{V^e} [B]^T[D][B]dV\right) \quad (24)$$

$$[K_e]=t.[C]^{-T}\left(\int\int [Q]^T\cdot[D]\cdot[Q]dxdy\right)[C]^{-1} \quad (25)$$

where *t* is the thickness:

$$[K_e]=t.[C]^{-T}[K_0][C]^{-1} \quad (26)$$

$$[K_0]=\int\int [Q]^T\cdot[D]\cdot[Q]dxdy \quad (27)$$

Using numerical integration:

$$[K_0]=\int_{-1}^{1}\int_{-1}^{1} [Q]^T[D][Q]\det|J|d\xi d\eta \quad (28)$$

where *J* presents the Jacobean. The element nodal body forces vector is:

$$\{F_b\}=\int_{V^e} [N]^T\{f_v\}dV=[C]^{-T}\left(\int_{V^e} [P]^T\{f_v\}dV\right) \quad (29)$$

After assembly over all elements, the global stiffness *[K]* is used in global equations for static, given as:

$$[K]\{q\}=[F] \quad (30)$$

B. *Case of Axisymmetric Formulation*

The strain components in the case of axisymmetric formulation are given as:

$$\begin{cases}\varepsilon_r=\dfrac{\partial u}{\partial r}\\ \varepsilon_z=\dfrac{\partial v}{\partial z}\\ \gamma_{rz}=\dfrac{\partial u}{\partial z}+\dfrac{\partial v}{\partial r}\\ \varepsilon_\theta=\dfrac{u}{r}\end{cases} \quad (31)$$

and the element stiffness matrix in the axisymmetric case is:

$$[K_e]=\left(\int_{V^e} [B]^T[D][B]r.\,dV\right) \quad (32)$$

where *r* is the radial coordinate, and *[D]* is the axisymmetric elasticity matrix given in the Appendix. It is worth noting here that the integrals calculations in the used programs use the Gauss numerical integration. In the case of forced vibration, the complex response method is used [48].

III. NUMERICAL VALIDATION

Several tests were selected to evaluate the accuracy of the element with different analyses such as plane strain, plane stress, axisymmetric, and dynamic. A comparative study was conducted between the proposed and the following elements:

TABLE I. ELEMENTS USED IN THE COMPARATIVE STUDY

SBQM [19]	5-node quadrilateral element with in-plane rotation based on the strain approach.
Q4	Standard four-node quadrilateral element.
Q8	Standard eight-node quadrilateral element.
Q6 [20]	Quadrilateral element with six nodes.
FRQ [10]	4-node quadrilateral element based on the "Plane Fiber Rotation" concept.
Q4WT [21]	Quadrilateral element with four nodes with incompatible modes.
Q4PS [21]	4-node quadrilateral hybrid element.
CPS8 [19]	Classic 8-node quadrilateral element in-plane stress with exact integration (Abaqus).
SBRIEIR [40]	Element with strain field at four nodes with in-plane rotation.
Q4CST [20]	The constant strain quadrilateral.
QM5 [20]	Plane stress element and Verbeke plate element boundary element formulation.
SBQ5 [41]	Strain-based quadrilateral element with five nodes.
SBE [42]	Strain Based Element.
CQUAD4 [43]	MSC/NASTRAN

A. *Linear Elasticity Tests*

1) *Macneal's Beam*

The sensitivity of the proposed element to mesh distortion was evaluated using the Macneal beam. Three distinct meshes (rectangular, parallelogram, and trapezoidal) were adopted. The Macneal and Harder test [44] is well-known as the standard for testing the mesh distortion sensitivity. There were two loading cases under consideration: pure bending and transverse linear bending. Figure 2 shows the appropriate mechanical and geometrical data, while Tables II and III show the results obtained by the proposed versus the other elements.

TABLE II. NORMALIZED DEFLECTION FOR MACNEAL'S ELONGATED BEAM SUBJECTED TO END SHEAR

Element	**Force shearing at the free end P=1**		
	Mesh Type		
	Rectangular (a)	**Parallelogram (b)**	**Trapezoidal (c)**
SBQM [19]	0.993	0.964	0.972
Q4	0.093	0.035	0.003
Q8	0.951	0.919	0.854
SBE [42]	1	0.976	0.978
SBFN	**0.993**	**0.993**	**0.994**
Reference solution [44]	**- 0.1081**		

TABLE III. NORMALIZED DEFLECTION FOR MACNEAL'S ELONGATED BEAM SUBJECTED TO END PURE BENDING

Element	Pure bending moment M=0.2		
	Mesh Type		
	Rectangular (a)	Parallelogram (b)	Trapezoidal (c)
SBQM [19]	1	1	1
Q4	0.093	0.031	0.022
Q8	1	0.994	0.939
SBE [42]	1	0.989	0.989
SBFN	**1**	**1**	**1**
Reference solution [44]	**− 0.0054**		

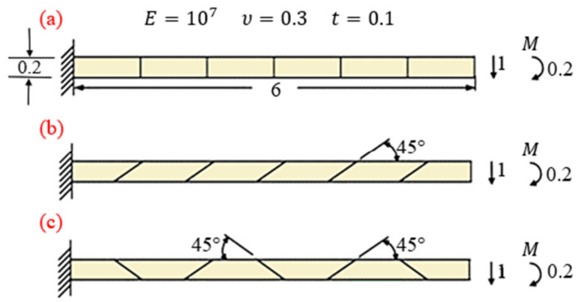

Fig. 2. McNeal's cantilever beam: (a) rectangular (b) trapezoidal (c) parallelogram.

Low sensitivity to mesh distortion was observed for the strain-based elements SBQM, SBE, and for the standard eight-node quadrilateral element Q8 for both loading cases in trapezoidal and parallelogram mesh. A neglected sensitivity in all mesh types was registered for the SBFN element, and more accuracy was observed in cases (b) and (c) compared to the other elements. However, the transverse shears locking resulting from over rigidity of the standard four-node quadrilateral element Q4 affected its results.

2) Beam In-Plane Bending

The proposed element was validated in the console beam problem subjected to a uniform vertical load using [21] and [10]. The vertical displacement at the beam's free end was computed using five meshes, as shown in Figure 3. Timoshenko's beam theory was implemented for a reference solution:

$$V_c^{ref} = \frac{L^3}{3EI} + \frac{6P_zL}{5GA} \quad (33)$$

Table IV shows the results obtained from the SBFN element for several meshes (M1, M2, M3, M4, and M5). The obtained results were compared to some other membrane element outcomes, allowing to note the following:

- SBFN gave more accurate results than the Q4, FRQ, and SBRIEIR elements.
- Similar results were noticed for Q4WT, Q4PS, and Q8 elements for regular meshes M1, M2, and M3.
- The SBFN element was more insensitive to distorted meshes than other membrane elements for M4 and M5 meshes.

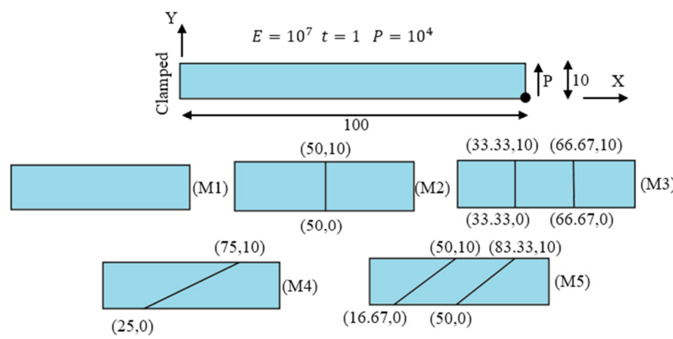

Fig. 3. Beam in-plane bending (data and meshes).

TABLE IV. VERTICAL DISPLACEMENT OF A BEAM IN PLANE BENDING

Mesh Type	FRQ [10]	Q4 [21]	Q4WT [21]	Q4PS [21]	Q8 [21]	SBRIEIR [19]	SBQM [19]	SBFN
M1	2.76	0.10	3.03	3.03	3.03	2.86	3.02	**3.03**
M2	3.44	0.38	3.78	3.78	3.7	3.57	3.77	**3.78**
M3	3.56	0.75	3.92	3.92	3.84	3.71	3.91	**3.91**
M4	1.09	0.12	0.30	0.49	0.64	2.92	3.04	**4.53**
M5	1.61	0.22	1.79	1.94	1.76	3.04	3.14	**4.27**
Reference solution [21]		**4.03**						

3) Cook's Skew Beam

The non-prismatic beam is a popular benchmark problem for evaluating planar elements. Several studies [45-57] have treated this problem. Due to the lack of an analytical solution, the reference solution was obtained using the CPS8 element of ABAQUS with a 64×64 mesh. The mechanical properties, the geometrical, and the loading data used in the treated structure are presented in Figure 4. The results of the vertical deflection at point *C* are shown in Table V. The SBFN element provided a good agreement with the reference solution, although the mesh was coarse compared to the Q4, SSQUAD [14], CQUAD4 [43], SBQM [19], and CPS8 [19] elements.

TABLE V. TIP VERTICAL DEFLECTION OF THE COOK'S SKEW BEAM

	Mesh -Vertical displacement at point C			
Element	2×2	4×4	8×8	16×16
Q4	11.80	18.29	22.08	23.43
SSQUAD [14]	25.65	24.27	24.01	23.96
CQUAD4 [43]	21.05	23.02	23.69	23.94
SBQM [19]	23.2173	23.4350	23.7376	23.9817
CPS8 [19]	23.35	24.54	23.8793	23.8596
SBFN	**23.9298**	**23.9282**	**23.9267**	**23.9411**
Reference solution [48]	**23.9652**			

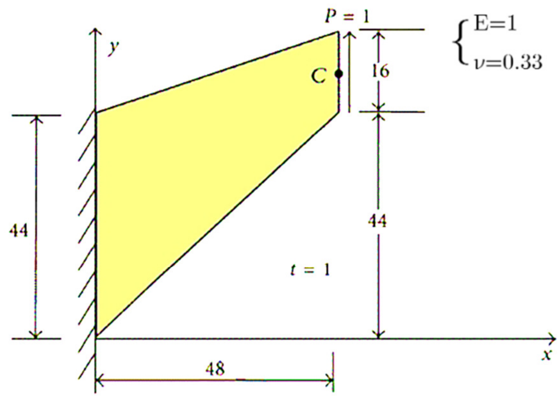

Fig. 4. Cook's skew beam.

B. *Axisymmetric Elasticity Test*

1) Simply Supported Circular Plate Uniformly Loaded

A simply supported circular plate under uniform load having a thickness t=1 was considered. Two distinguishable meshes were used for the discretization of the plate. At first, a rectangular mesh with a distortion e=0 followed by a trapezoidal mesh with a distortion e=0.025 was applied, as shown in Figure 5. The exact solution was taken from [49] as:

$$w(r)=\frac{p\cdot r_0^4}{64\cdot D(1+\upsilon)}\left[2\cdot(3\upsilon)\cdot\left(1-\left(\frac{r}{r_0}\right)^2\right)-(1+\upsilon)\cdot\left(1-\left(\frac{r}{r_0}\right)^4\right)\right] \quad (34)$$

$$\begin{cases} w_{max}=w(0) \\ w_{max}=\frac{p\cdot r_0^4(5+\upsilon)}{64\cdot D\cdot(1+\upsilon)} \end{cases} \quad (35)$$

where p and r_0 are respectively the uniform load and radius of the plate, and D is the flexural rigidity expressed as:

$$D=\frac{Eh^3}{12(1-2\nu)} \quad (36)$$

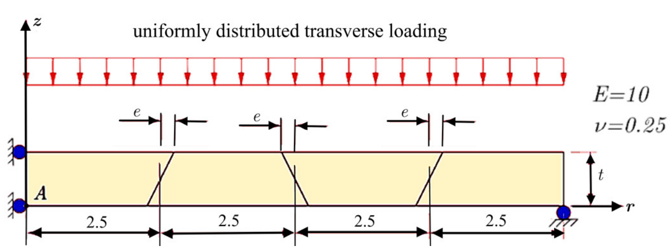

Fig. 5. Simply supported uniformly loaded circular plate.

TABLE VI. NORMALIZED VERTICAL DISPLACEMENT AT THE CENTER 'A' FOR THE UNIFORMLY LOADED CIRCULAR PLATE

	Mesh type - u_{zA}	
Element	**Rectangular**	**Trapezoidal**
Q4	0.696	0.694
Q8	1.0079	1.0183
SBFN	0.9889	0.989
Reference solution [49]	−738.280	

Table VI shows the obtained results of displacement. It can be noted that the SBFN element gave excellent results close to the exact solution, similar to those provided by the Q8 element, whereas the Q4 element gave poor results. The SBFN element gave the best results for the cases where bending was dominant.

1) Axisymmetric Cylindrical Shell

A thin cylindrical shell R/e = 168 was subjected to a moment in the end [20], as shown in Figure 6. This is a problem of a thin shell with axisymmetric loading where the exact solution can be found using the theory of shells in the infinite length case. A quadrilateral element through the thickness was used. The result of the theoretical solution of the shells [49] was used to compare with the numerical radial displacement for the formulated and various types of elements. The obtained results are shown in Table VII and Figure 7. The formulated element provided excellent results, which will be more pronounced in bending cases.

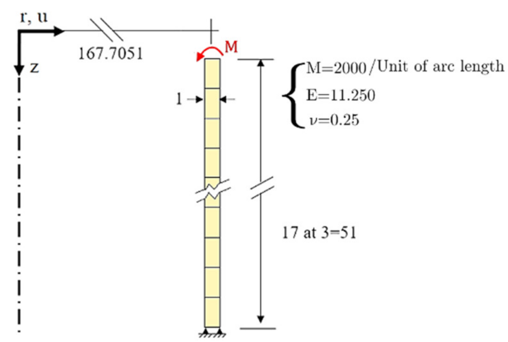

Fig. 6. Cylindrical shell analysis.

TABLE VII. RADIAL DISPLACEMENTS (U) FOR THE AXISYMMETRIC CYLINDRICAL SHELL

	Radial displacements u					
Z	**Q4CST [19]**	**QM5 [19]**	**Q4 [19]**	**Q6 [19]**	**SBFN**	**Analytical solution [19]**
0	39.97	98.56	46.47	100.01	**100.08**	**100.00**
3	26.04	47.87	29.17	48.98	**49.01**	**48.88**
6	14.98	13.49	15.69	14.19	**14.40**	**14.31**
9	6.56	-7.29	5.69	-6.54	**-6.54**	**-6.57**
12	0.47	-17.77	-1.31	-17.15	**-17.17**	**-17.16**
15	-3.65	-21.17	-5.82	-20.70	**-20.72**	**-20.68**
18	-6.16	-20.21	-8.35	-19.88	**-19.90**	**-19.85**
21	-7.40	-16.97	-9.39	-16.83	**-16.80**	**-16.75**
24	-7.68	-12.92	-9.33	-12.85	**-12.86**	**-12.82**
27	-7.27	-8.98	-8.55	-9.00	**-9.01**	**-8.95**
30	-6.40	-5.65	-7.32	-5.72	**-5.73**	**-5.63**
33	-5.27	-3.12	-5.87	-3.23	**-3.24**	**-3.06**

The obtained results clearly show that the Q4 and Q4CST elements gave very erroneous values. These elements have difficulty representing the bending phenomena. SBFN, QM5, and Q6 showed very good levels of accuracy with the theoretical solution. The excellent results are remarkable for the formulated element in the case where bending is predominant.

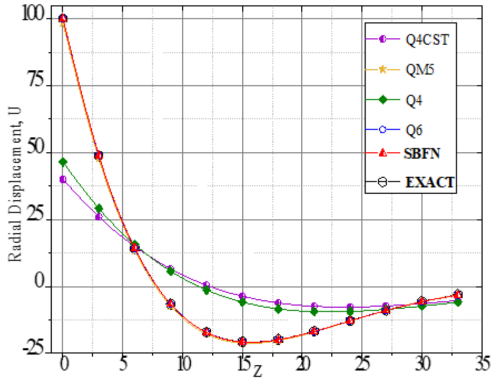

Fig. 7. Radial displacements (u) for the axisymmetric cylindrical shell.

C. Dynamic Numerical Validation

1) Forced Vibration of a Rectangular Solid in-Plane Strain

This benchmark tested the proposed element in a rectangular beam in-plane strain case to analyze forced vibrations using the complex response method. The modeled results were compared with those obtained by Q8 [50] and Q4, SBQ5, and SBRIE [41]. Fig. 9. Figure 8 shows the geometric components of the evaluated beam and its mechanical properties. The beam was subjected to a vertical harmonic force $F=cos(\omega t)$, where force-frequency was 0.3, time step was 1/20, the period was 2π/ω, and the ratio of depreciation was 5%. Figure 9 shows the displacements for step time results. It is noticed that the proposed SBFN agreed well with the Q8 element.

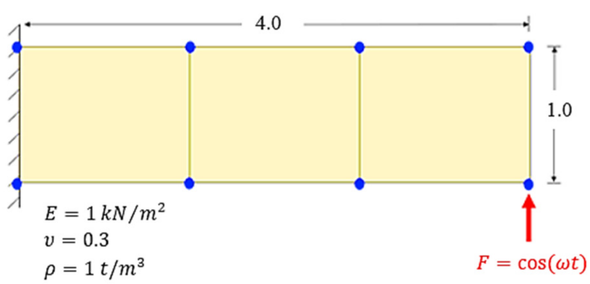

Fig. 8. Geometrical and mesh presentation of the console beam subjected to forced vibration.

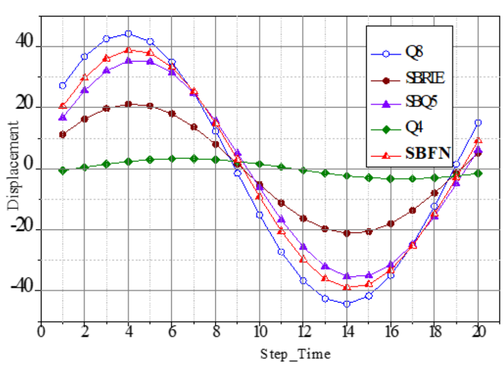

Fig. 9. Displacement as a function of time for a console beam.

IV. CONCLUSION

This study proposed a new quadrilateral plane element using an assumed strain approach. Rigid body motions, constant strain, and application of compatibility conditions to the assumed strain field guaranteed and optimized monotonic convergence to the solution. The formulated element had five nodes with eleven degrees of freedom, whereas the fifth node of the element was located in the center having three degrees of freedom (u, v, θ). This central node was eliminated using the static condensation method. Therefore, the proposed became a simple four-node element with two essential degrees of freedom (u, v) in each of the four corner nodes. The SBFN linear quadrilateral element showed acceptable performance, was insensitive to mesh distortion, and had an excellent convergence characteristic in all numerical examples. The proposed membrane element's precision was often close to that of the second-order quadrilateral plane element Q8, in static and dynamic analysis for plane and axisymmetric structures. Furthermore, the obtained numerical results of the proposed element were consistent and give better results when bending dominated.

APPENDIX

For the case of plane stress problem, the elasticity matrix [D] is:

$$[D] = \frac{E}{(1-v^2)}\begin{bmatrix} 1 & v & 0 \\ v & 1 & 0 \\ 0 & 0 & \frac{1-v}{2} \end{bmatrix} \quad (A.1)$$

For the case of plane strain problem, the elasticity matrix [D] is:

$$[D] = \frac{E}{(1+v)(1-2v)}\begin{bmatrix} (1-v) & v & 0 \\ v & (1-v) & 0 \\ 0 & 0 & \frac{(1-2v)}{2} \end{bmatrix} \quad (A.2)$$

For the case of axisymmetric problem, the elasticity matrix [D] is:

$$[D] = \frac{E(1-v)}{(1+v)(1-2v)}\begin{bmatrix} 1 & \frac{v}{1-v} & \frac{v}{1-v} & 0 \\ \frac{v}{1-v} & 1 & \frac{v}{1-v} & 0 \\ \frac{v}{1-v} & \frac{v}{1-v} & 1 & 0 \\ 0 & 0 & 0 & \frac{1-2v}{2(1-v)} \end{bmatrix} \quad (A.3)$$

REFERENCES

[1] A. G. da S. Jr, J. A. Martins, and E. C. Romão, "Numerical Simulation of a One-Dimentional Non-Linear Wave Equation," *Engineering, Technology & Applied Science Research*, vol. 12, no. 3, pp. 8574–8577, Jun. 2022, https://doi.org/10.48084/etasr.4920.

[2] F. Khelil, M. Belhouari, N. Benseddiq, and A. Talha, "A Numerical Approach for the Determination of Mode I Stress Intensity Factors in PMMA Materials," *Engineering, Technology & Applied Science Research*, vol. 4, no. 3, pp. 644–648, Jun. 2014, https://doi.org/10.48084/etasr.442.

[3] A. Boulenouar, N. Benseddiq, and M. Mazari, "Two-dimensional Numerical Estimation of Stress Intensity Factors and Crack Propagation in Linear Elastic Analysis," *Engineering, Technology & Applied Science Research*, vol. 3, no. 5, pp. 506–510, Oct. 2013, https://doi.org/10.48084/etasr.363.

[4] M. J. Turner, R. W. Clough, H. C. Martin, and L. J. Topp, "Stiffness and Deflection Analysis of Complex Structures," *Journal of the Aeronautical Sciences*, vol. 23, no. 9, pp. 805–823, 1956, https://doi.org/10.2514/8.3664.

[5] I. C. Taig and R. I. Kerr, "Some Problems in the Discrete Element Representation of Aircraft Structures," in *Matrix Methods of Structural Analysis*, F. de Veubeke, Ed. Oxford, UK: Pergamon Press, 1964, pp. 267–316.

[6] K. Y. Sze, "On immunizing five-beta hybrid-stress element models from 'trapezoidal locking' in practical analyses," *International Journal for Numerical Methods in Engineering*, vol. 47, no. 4, pp. 907–920, 2000, https://doi.org/10.1002/(SICI)1097-0207(20000210)47:4<907::AID-NME808>3.0.CO;2-A.

[7] W. Chen and Y. K. Cheung, "Axisymmetric solid elements by the generalized hybrid method," *Computers & Structures*, vol. 27, no. 6, pp. 745–752, Jan. 1987, https://doi.org/10.1016/0045-7949(87)90287-2.

[8] K. Y. Sze and C. L. Chow, "An incompatible element for axisymmetric structure and its modification by hybrid method," *International Journal for Numerical Methods in Engineering*, vol. 31, no. 2, pp. 385–405, Feb. 1991, https://doi.org/10.1002/nme.1620310211.

[9] F. Boussem and L. Belounar, "A Plate Bending Kirchhoff Element Based on Assumed Strain Functions," *Journal of Solid Mechanics*, vol. 12, no. 4, pp. 935–952, Dec. 2020, https://doi.org/10.22034/jsm.2020.1901430.1601.

[10] R. Ayad, "Éléments finis de plaque et coque en formulation mixte avec projection en cisaillement," Ph.D. dissertation, University of Compiègne, 1993.

[11] K. Guerraiche, "Elements finis d'Elasticite Plane et de Volume Bases Sur l'Approche en Defomation," Ph.D. dissertation, University Mohamed Khider - Biskra, 2014.

[12] Y. Long and Y. Xu, "Generalized conforming quadrilateral membrane element with vertex rigid rotational freedom," *Computers & Structures*, vol. 52, no. 4, pp. 749–755, Aug. 1994, https://doi.org/10.1016/0045-7949(94)90356-5.

[13] W. Changsheng, Q. Zhaohui, Z. Xiangkui, and H. Ping, "Quadrilateral 4-node Quasi-Conforming Plane Element with Internal Parameters," *Chinese Journal of Theoritical and Applied Mechanics*, vol. 46, no. 6, pp. 971–976, Nov. 2014, https://doi.org/10.6052/0459-1879-14-167.

[14] M. Rezaiee-Pajand and M. Yaghoobi, "Formulating an effective generalized four-sided element," *European Journal of Mechanics - A/Solids*, vol. 36, pp. 141–155, Nov. 2012, https://doi.org/10.1016/j.euromechsol.2012.02.012.

[15] M. S. Djoudi and H. Bahai, "A cylindrical strain-based shell element for vibration analysis of shell structures," *Finite Elements in Analysis and Design*, vol. 40, no. 13, pp. 1947–1961, Aug. 2004, https://doi.org/10.1016/j.finel.2003.11.008.

[16] A. B. Sabir and A. C. Lock, "A curved, cylindrical shell, finite element," *International Journal of Mechanical Sciences*, vol. 14, no. 2, pp. 125–135, Feb. 1972, https://doi.org/10.1016/0020-7403(72)90093-8.

[17] D. G. Ashwell, A. B. Sabir, and T. M. Roberts, "Further studies in the application of curved finite elements to circular arches," *International Journal of Mechanical Sciences*, vol. 13, no. 6, pp. 507–517, Jun. 1971, https://doi.org/10.1016/0020-7403(71)90038-5.

[18] A. B. Sabir and A. Sfendji, "Triangular and rectangular plane elasticity finite elements," *Thin-Walled Structures*, vol. 21, no. 3, pp. 225–232, Jan. 1995, https://doi.org/10.1016/0263-8231(94)00002-H.

[19] A. Belounar, "Eléments finis membranaires et flexionnels à champ de déformation pour l'analyse des structures," Ph.D. dissertation, University Mohamed Khider - Biskra, 2019.

[20] S. J. Fenves, N. Perrone, and A. R. Robinson, *Numerical and Computer Methods in Structural Mechanics*. New York, NY, USA: Elsevier, 2014.

[21] J.-L. Batoz and G. Dhatt, *Modélisation des structures par éléments finis*. Sainte-Foy, France: Presses Université Laval, 1990.

[22] M. Rezaiee-Pajand, N. Gharaei-Moghaddam, and M. Ramezani, "Review of the strain-based formulation for analysis of plane structures Part II: Evaluation of the numerical performance," *Iranian Journal of Numerical Analysis and Optimization*, vol. 11, no. 2, pp. 485–511, Sep. 2021, https://doi.org/10.22067/ijnao.2021.70940.1051.

[23] D. Boutagouga, "A Review on Membrane Finite Elements with Drilling Degree of Freedom," *Archives of Computational Methods in Engineering*, vol. 28, no. 4, pp. 3049–3065, Jun. 2021, https://doi.org/10.1007/s11831-020-09489-z.

[24] M. T. Belarbi and A. Charif, "Développement d'un nouvel élément hexaédrique simple basé sur le modèle en déformation pour l'étude des plaques minces et épaisses," *Revue Européenne des Éléments Finis*, vol. 8, no. 2, pp. 135–157, Jan. 1999, https://doi.org/10.1080/12506559.1999.10511361.

[25] K. Guerraiche, L. Belounar, and L. Bouzidi, "A New Eight Nodes Brick Finite Element Based on the Strain Approach," *Journal of Solid Mechanics*, vol. 10, no. 1, pp. 186–199, Mar. 2018.

[26] L. Belounar and K. Guerraiche, "A new strain based brick element for plate bending," *Alexandria Engineering Journal*, vol. 53, no. 1, pp. 95–105, Mar. 2014, https://doi.org/10.1016/j.aej.2013.10.004.

[27] L. Belounar and M. Guenfoud, "A new rectangular finite element based on the strain approach for plate bending," *Thin-Walled Structures*, vol. 43, no. 1, pp. 47–63, Jan. 2005, https://doi.org/10.1016/j.tws.2004.08.003.

[28] F. Boussem, A. Belounar, and L. Belounar, "Assumed strain finite element for natural frequencies of bending plates," *World Journal of Engineering*, vol. ahead-of-print, no. ahead-of-print, Jan. 2021, https://doi.org/10.1108/WJE-02-2021-0114.

[29] A. Belounar, F. Boussem, M. N. Houhou, A. Tati, and L. Fortas, "Strain-based finite element formulation for the analysis of functionally graded plates," *Archive of Applied Mechanics*, vol. 92, no. 7, pp. 2061–2079, Jul. 2022, https://doi.org/10.1007/s00419-022-02160-y.

[30] A. Belounar, S. Benmebarek, and L. Belounar, "Strain based triangular finite element for plate bending analysis," *Mechanics of Advanced Materials and Structures*, vol. 27, no. 8, pp. 620–632, Apr. 2020, https://doi.org/10.1080/15376494.2018.1488310.

[31] M. S. Djoudi and H. Bahai, "A shallow shell finite element for the linear and non-linear analysis of cylindrical shells," *Engineering Structures*, vol. 25, no. 6, pp. 769–778, May 2003, https://doi.org/10.1016/S0141-0296(03)00002-6.

[32] M. Bourezane M, "An Efficient Strain Based Cylindrical Shell Finite Element," *Journal of Solid Mechanics*, vol. 9, no. 3, pp. 632–649, Jan. 2017.

[33] A. Mousa, "Strain-Based Finite Element Analysis of Stiffened Cylindrical Shell Roof," *American Journal of Civil Engineering*, vol. 5, no. 4, Jul. 2017, https://doi.org/10.11648/j.ajce.20170504.15.

[34] H. Guenfoud, M. Himeur, H. Ziou, and M. Guenfoud, "A consistent triangular thin flat shell finite element with drilling rotation based on the strain approach," *International Journal of Structural Engineering*, vol. 9, no. 3, 2018, https://doi.org/10.1504/IJSTRUCTE.2018.093673.

[35] A. B. Sabir and M. S. Djoudi, "Shallow shell finite element for the large deflection geometrically nonlinear analysis of shells and plates," *Thin-Walled Structures*, vol. 21, no. 3, pp. 253–267, Jan. 1995, https://doi.org/10.1016/0263-8231(94)00005-K.

[36] C. Rebiai and L. Belounar, "A new strain based rectangular finite element with drilling rotation for linear and nonlinear analysis," *Archives of Civil and Mechanical Engineering*, vol. 13, no. 1, pp. 72–81, Mar. 2013, https://doi.org/10.1016/j.acme.2012.10.001.

[37] A. Belounar, L. Belounar, and A. Tati, "An assumed strain finite element for composite plates analysis," *International Journal of Computational Methods*, Jul. 2022, https://doi.org/10.1142/S0219876222500347.

[38] A. Belounar, F. Boussem, and A. Tati, "A Novel C0 Strain-Based Finite Element for Free Vibration and Buckling Analyses of Functionally Graded Plates," *Journal of Vibration Engineering & Technologies*, Jun. 2022, https://doi.org/10.1007/s42417-022-00577-x.

[39] M. Rezaiee-Pajand, N. Gharaei-Moghaddam, and M. Ramezani, "Strain-based plane element for fracture mechanics' problems," *Theoretical and Applied Fracture Mechanics*, vol. 108, Aug. 2020, Art. no. 102569, https://doi.org/10.1016/j.tafmec.2020.102569.

[40] A. B. Sabir, "A Rectangular and Triangular Plane Elasticisy Elements with Drilling Degrees of Freedom," in *Proceedings of the Second International Conference on Variational Methods in Engineering*, 1985, pp. 17–25.

[41] L. Bouzidi, L. Belounar, and K. Guerraiche, "Presentation of a new membrane strain-based finite element for static and dynamic analysis," *International Journal of Structural Engineering*, vol. 10, no. 1, pp. 40–60, Jan. 2019, https://doi.org/10.1504/IJSTRUCTE.2019.101431.

[42] C. Rebiai, N. Saidani, and E. Bahloul, "A New Finite Element Based on the Strain Approach for Linear and Dynamic Analysis," *Research Journal of Applied Sciences, Engineering and Technology*, vol. 11, no. 6, pp. 639–644, Jul. 2015.

[43] R. Winkler and D. Plakomytis, "A New Shell Finite Element with Drilling Degrees of Freedom and its Relation to Existing Formulations," in *Proceedings of the VII European Congress on Computational Methods in Applied Sciences and Engineering (ECCOMAS Congress 2016)*, Crete Island, Greece, 2016, pp. 2803–2842, https://doi.org/10.7712/100016.1998.11192.

[44] R. H. Macneal and R. L. Harder, "A proposed standard set of problems to test finite element accuracy," *Finite Elements in Analysis and Design*, vol. 1, no. 1, pp. 3–20, Apr. 1985, https://doi.org/10.1016/0168-874X(85)90003-4.

[45] Y. K. Cheung, Y. X. Zhang, and W. J. Chen, "A refined nonconforming plane quadrilateral element," *Computers & Structures*, vol. 78, no. 5, pp. 699–709, Dec. 2000, https://doi.org/10.1016/S0045-7949(00)00049-3.

[46] W. Zouari, F. Hammadi, and R. Ayad, "Quadrilateral membrane finite elements with rotational DOFs for the analysis of geometrically linear and nonlinear plane problems," *Computers & Structures*, vol. 173, pp. 139–149, Sep. 2016, https://doi.org/10.1016/j.compstruc.2016.06.004.

[47] P. G. Bergan and C. A. Felippa, "A triangular membrane element with rotational degrees of freedom," *Computer Methods in Applied Mechanics and Engineering*, vol. 50, no. 1, pp. 25–69, Jul. 1985, https://doi.org/10.1016/0045-7825(85)90113-6.

[48] R. D. Cook, D. S. Malkus, M. E. Plesha, and R. J. Witt, *Concepts and Applications of Finite Element Analysis, 4th Edition*. Hoboken, NJ, USA: John Wiley & Sons, Ltd, 2001.

[49] S. Timoshenko and S. Woinowsky-krieger, *Theory of Plates and Cells*. New York, NY, USA: Mc Graw-Hill, 1959.

[50] I. M. Smith, D. V. Griffiths, and L. Margetts, *Programming the Finite Element Method*. Chichester, UK: John Wiley & Sons, 2013.